JOURNAL OF VIROLOGY, June 2005, p. 7113–7120 Vol. 79, No. 11
0022-538X/05/$08.00+0 doi:10.1128/JVI.79.11.7113–7120.2005


# Viral Expression of CCL2 Is Sufficient To Induce Demyelination in RAG1$^{-/-}$ Mice Infected with a Neurotropic Coronavirus

Taeg S. Kim[1] and Stanley Perlman[1,2]*

*Interdisciplinary Program in Immunology[1] and Departments of Pediatrics and Microbiology,[2] University of Iowa, Iowa City, Iowa 52242*

Received 10 December 2004/Accepted 19 January 2005

**Mouse hepatitis virus strain JHM causes a chronic demyelinating disease in susceptible strains of rodents. Demyelination does not develop in infected RAG1$^{-/-}$ (recombination activation gene-deficient) mice but can be induced by several experimental interventions, including adoptive transfer of virus-specific T cells or antibodies. A common feature of demyelination in these models is extensive infiltration of macrophages/microglia into the white matter. The data obtained thus far do not indicate whether macrophage/microglia infiltration, in the absence of T cells or antibody, is sufficient to mediate demyelination. To determine whether the expression of a single macrophage chemoattractant, in the context of virus infection, could initiate the demyelinating process, we engineered a recombinant coronavirus that expressed the chemokine CCL2/monocyte chemoattractant protein-1. CCL2 has been implicated in macrophage infiltration into the central nervous system and is involved in demyelination in many experimental models of demyelination. Extensive macrophage/microglia infiltration and demyelination has developed in RAG1$^{-/-}$ mice infected with this recombinant virus. Thus, these results suggest that the minimal requirement for demyelination is increased expression of a single macrophage-attracting chemokine in the context of an inflammatory milieu, such as that induced by a viral infection.**

Demyelination accompanied by the extensive infiltration of inflammatory cells is characteristically observed in humans with multiple sclerosis and in rodents with experimental autoimmune encephalomyelitis (EAE) or those infected with viruses such as Theiler's encephalomyelitis virus or mouse hepatitis virus (18, 45). The inflammatory infiltrate consists, in general, of lymphocytes and macrophages. The mechanism used by these cells to enter the central nervous system (CNS) has been partly elucidated (reviewed in reference 41). Several chemokines, including CCL2/monocyte chemoattractant protein-1 (MCP-1), CCL3/MIP-1α, CCL5/RANTES, CXCL9/Mig, and CXCL10/IP-10, are upregulated in the inflamed CNS (22, 44) and are involved in T-cell or monocyte/macrophage infiltration. Of the macrophage chemoattractants, CCL2 has been most extensively studied (21, 30). CCL2 is detected at early times in mice with EAE, but its expression is not one of the initial steps in this process (12). Rather, CCL2 expression follows the infiltration of antigen-specific T cells, suggesting that it contributes to amplification of the inflammatory process. The importance of CCL2 in EAE was shown in experiments in which mice deficient in CCL2 or CCR2 expression developed less severe disease than did their wild-type counterparts (21).

Mice infected with the JHM strain of mouse hepatitis virus, including the attenuated variant J2.2-v-1, develop acute encephalitis and acute and chronic demyelinating encephalomyelitis (33). Demyelination is largely immune mediated, because sublethally irradiated or congenitally immunodeficient mice, when infected with J2.2-v-1, develop acute encephalitis but not demyelination (19, 52, 55). Transfer of splenocytes from JHM-immune mice to infected RAG1$^{-/-}$ mice (mice deficient in recombination activation gene 1) results in demyelination within 7 days (55). α/β T cells are not absolutely required for demyelination in this system because demyelination also occurs, albeit with slower kinetics, when anti-JHM antibody is transferred to infected RAG1$^{-/-}$ mice (24). CCL2, like several other chemokines including CXCL10 and CCL5, has been detected in the CNS of J2.2-v-1-infected RAG1$^{-/-}$ mice in the absence of the adoptive transfer of either anti-JHM T cells or antibody (16, 37, 39, 54). Its expression did not increase to a significant extent after the adoptive transfer of cells or antibody. However, experiments using mice in which the function of CCL2, CCL3, CCL5, CXCL9, or CXCL10 was disrupted revealed essential and nonredundant roles for these chemokines in T-cell and macrophage recruitment into the CNS, virus clearance, and demyelination (3, 27–29, 47).

One possibility is that the interaction of virus-specific T cells or antibody with infected cells in RAG1$^{-/-}$ mice results in the localized release of a macrophage/microglia chemoattractant(s) and that this molecule(s), by itself, is sufficient to initiate the cascade of events leading to demyelination. If this were the case, no component of the adaptive immune response would be required, provided that the appropriate macrophage chemoattractant was expressed at high levels in infected cells. Since such a chemokine has not yet been identified in JHM-infected mice, we examined this possibility by infecting RAG1$^{-/-}$ mice with a recombinant J2.2-v-1 engineered to express CCL2.

* Corresponding author. Mailing address: Department of Pediatrics, University of Iowa, Medical Laboratories 2042, Iowa City, IA 52242. Phone: (319) 335-8549. Fax: (319) 335-8991. E-mail: Stanley-Perlman@uiowa.edu.

## MATERIALS AND METHODS

**Virus and cells.** Virus was grown and titered as described previously (34). A recombinant strain of JHM, encoding the feline surface (S) glycoprotein (des-

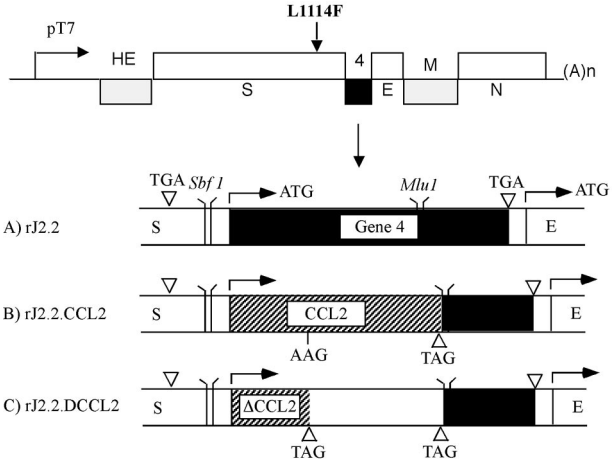


FIG. 1. Schematic diagram of recombinant J2.2 virus constructions. (A) Recombinant J2.2-v-1 (rJ2.2) was generated as described in Materials and Methods. (B) To engineer a recombinant virus that expressed CCL2, a CCL2-specific PCR product was cloned from RNA harvested from bone marrow cells and inserted into gene 4 of rJ2.2 using SbfI and MluI restriction sites. (C) As a control, a virus that encoded a truncated CCL2 protein was also generated (lys [AAG] to stop codon [TAG] at residue 52; rJ2.2.ΔCCL2).

ignated fMHV-JHM clone B3b), was propagated in AK-D (feline) cells as described previously (32). THP-1 human promonocytic cells were maintained in RPMI-1640 containing 10% fetal calf serum and antibiotics.

**Animals.** Specific-pathogen-free RAG1$^{-/-}$ mice were purchased from Jackson Laboratories (Bar Harbor, ME) and bred at the University of Iowa (Iowa City, IA). Six- to eight-week-old RAG1$^{-/-}$ mice were inoculated intracerebrally (i.c.) with 500 PFU of rJ2.2, rJ2.2.CCL2, or rJ2.2.ΔCCL2 in 30 μl of Dulbecco's modified Eagle medium. Virus was harvested from the infected CNS and titered by plaque assay as described previously (34). All animal studies were approved by the University of Iowa Animal Care and Use Committee.

**Preparation of cellular RNA and cDNA synthesis.** RNA was extracted from infected tissue cells or bone marrow-derived cells, and cDNA was synthesized from 2 μg total RNA as described previously (38).

**Recombinant viruses.** Targeted recombination was used to generate recombinant virus, as described elsewhere (25, 31, 32) and shown in Fig. 1. The attenuated J2.2-v-1 strain of JHM differs from JHM.SD (31) at a single amino acid within the S protein (L1114F) (51). To engineer a recombinant version of J2.2-v-1, a plasmid containing genes 2 to 7 of JHM.SD (pJHM.SD [31]) was modified to contain the L1114F mutation. For this purpose, a 1,310-bp product was generated by reverse transcription (RT)-PCR, using RNA harvested from cells infected with J2.2-v-1. The primers used for PCR encompassed nucleotides (nt) 2846 to 2871(5′-GT CAA GAA GT*T CGC GA*C CTC CTT TGC-3′; forward) and nt 4126 to 4156 (5′-G TCT TT*C CTG CAG G*GG CTG TGA TAG TCA ATC-3′; reverse) of the S gene. The forward and reverse primers contained the NruI and SbfI restriction sites (italicized), respectively, to allow subcloning into pJHM.SD. The resulting product was then introduced into pJHM.SD (pJ2.2).

We then introduced the *CCL2* gene into pJ2.2, replacing part of gene 4 as described previously (23) (Fig. 1). In brief, a CCL2-specific PCR product was cloned from RNA harvested from murine bone marrow cells. The primers used to clone the *CCL2* gene contained the JHM and CCL2 (underlined) sequences and Sbf1 and Mlu1 restriction sites (italicized, forward and reverse primers, respectively) as follows: 5′-C AGC C*CC TGC AGG* AAA GAC AGA AAA TCT AAA CAA TTT ATA GCA TTT TAG TTG CTA CTT TGC TCC TCT AGA GGG CAG CAA GTA GTT ATG CAG GTC CCT GTC ATG CTT CTG G-3′ (forward) and 5′-G CTT GCC AGT C*AC GCG T*AT GGT ATC CTT CTA GTT CAC TGT CAC ACT G-3′ (reverse). The cloned *CCL2* gene was introduced into pJ2.2 (designated pJ2.2.CCL2). As a control, an additional construct was developed in which the lys (**a**ag) residue at position 52 of the *CCL2* gene was mutated to a termination codon (**t**ag) using overlapping extension PCR with two sets of primers (designated pJ2.2.ΔCCL2). The inner primers for this construct were (point mutations in bold) as follows: 5′-GAG AGC TAC **T**AG AGG ATC ACC AGC AGC AG-3′ (forward) and 5′-GT GAT CCT CT**A** GTA GCT CTC CAG CCT ACT CAT TGG-3′ (reverse). Donor RNAs were transcribed using T7 polymerase and transfected into feline cells (AK-D) previously infected with fMHV-JHM. fMHV-JHM does not infect murine cells, but recombinant virus expressing the JHM S protein does, allowing for efficient selection of recombinant virus. Recombinant virus was then propagated as described previously (23, 25, 32). The presence of the introduced changes was confirmed by sequence analysis prior to use in further studies. To control for any unwanted mutations that might have occurred during the process of targeted recombination, at least two independent isolates of each recombinant virus were analyzed in these studies. Identical results were obtained with both isolates, and data from both isolates were combined in the studies described below.

**Detection of CCL2 and virus in infected cells by RT-PCR.** For the detection of CCL2 and viral RNA in infected tissue culture cells, sets of primers specific for the S protein (nt 690 to 714, 5′-G TAT ATT GGC GAC ATT TTA ACA AG-3′, and nt 1217 to 1240, 5′-C CGT TTG CAA AAA TCC GGA GTT GC-3′; 550 bp) or CCL2 (nt 19 to 45, 5′-CTT CTG GGC CTG CTG TTC ACA GTT GCC-3′, and nt 359 to 384, 5′-GGA TGC ATTAGCTTCAGATTT ACG G-3′; 366 bp) were used. To detect virus-expressed *CCL2* mRNA in mice, primers specific for virus sequences flanking the gene were developed (nt 4061 to 4082 of the S gene, 5′-GT TGT TGT GAT GAG TAT GGA GG-3′, and nt 261 to 278 of gene 4, 5′-CCT CTT GAA CTA CCA AGG-3′) and used in PCRs. The final PCR products were run on 1% agarose gels and sequenced at the DNA Sequencing Facility at the University of Iowa (Iowa City, IA).

**Transmigration assay.** The chemoattractant activity of virus-expressed CCL2 was measured as previously described (53), with modifications. Briefly, HeLa-MHVR cells were infected with rJ2.2, rJ2.2.CCL2, or rJ2.2.ΔCCL2 at a multiplicity of infection (MOI) of 0.5 PFU/cell for 4 h and then replaced with fresh Opti-MEM media (Gibco, Invitrogen, NY) for an additional 12 h. Supernatants were clarified and placed in the bottom well of a transwell plate (6.5 mm, 5-μm pore size; Corning, Corning, NY). Some supernatants were preincubated for 30 min with 100 μg/ml anti-CCL2 antibody (R&D Systems, Minneapolis, MN). Next, $5 \times 10^5$ THP-1 cells were incubated in the top chamber of the transwell plate at 37°C for 2 h. Following the migration period, adherent and nonadherent cells were collected from each chamber, pelleted by centrifugation ($500 \times g$, 5 min), and resuspended in 0.5 ml 2% formaldehyde—phosphate-buffered saline. The number of cells present in the lower chambers of the transwell plate was determined by counting each cell population for 1 min in a FACScan flow cytometer (BD Biosciences, Mountain View, CA). Each sample was analyzed in quadriplicate.

**Luxol Fast Blue staining and quantification of demyelination.** Demyelination was quantified as described previously (7).

**Immunohistochemistry.** Macrophages/microglia or viral antigens were detected using rat anti-F4/80 (CI:A3-1; Serotec, Oxford, England) or mouse anti-nucleocapsid (N) (monoclonal antibody [MAb] 5B188.2, provided by M. Buchmeier, The Scripps Research Institute), respectively, as described previously (7).

**Immunofluorescence assays.** HeLa-MHVR cells were seeded onto 4-well chamber slides (Lab-Tek, Nalge Nunc International Corp, IL) and infected with virus at an MOI of 0.1. After 4 h, GolgiPlug (BD Biosciences, San Diego, CA) was added and cells were incubated for an additional 4 h. Cells were fixed in cold methanol for 20 min at −20°C and washed three times with phosphate-buffered saline. Slides were blocked with 10% horse serum for 10 min and incubated overnight at 4°C with goat anti-mouse CCL2 antibody (1:200; R&D systems, Minneapolis, MN) and mouse anti-N MAb. Samples were then incubated successively with fluorescein isothiocyanate-conjugated anti-mouse immunoglobulin G (IgG; Jackson ImmunoResearch) and biotinylated rabbit anti-goat IgG antibody (Jackson ImmunoResearch), followed by streptavidin-Cy3 (Jackson ImmunoResearch). To detect phosphoneurofilament in tissues, zinc formalin-fixed sections were incubated with a cocktail of mouse anti-phosphoneurofilament MAbs (1:100, SMI-312; Sternberger Monoclonal antibodies, Lutherville, MD), followed by fluorescein isothiocyanate-conjugated anti-mouse IgG.

**Quantification of macrophages/microglia.** To quantify the number of macrophages/microglia in the CNS, we counted F4/80-positive cells in 1.25-mm-wide cross-sections at 10 levels within the gray and white matter of the midsagittal sections of spinal cords. Three mice infected with rJ2.2.CCL2 and three infected with rJ2.2.ΔCCL2 were examined.

**Statistics.** A two-tailed unpaired Student *t* test was used to analyze differences in mean values between groups. All results are expressed as means ± standard errors of the means. Values of $P < 0.05$ were considered statistically significant.

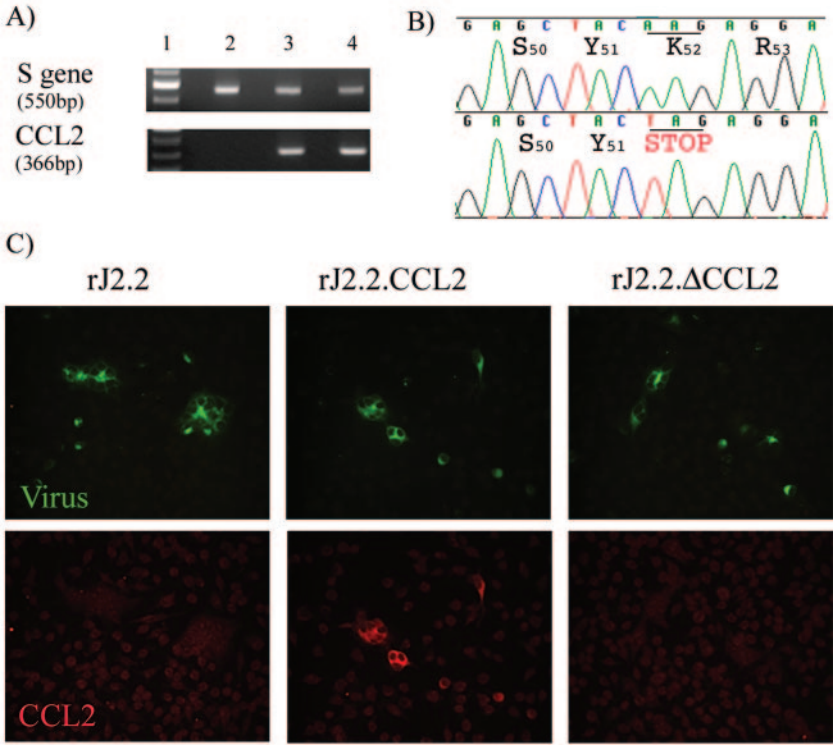


FIG. 2. Detection of *CCL2* mRNA and protein in HeLa-MHVR cells infected with rJ2.2.CCL2. (A) CCL2 expression in cells infected with rJ2.2, rJ2.2.CCL2, or rJ2.2.ΔCCL2 was examined at 16 h p.i. by RT-PCR and agarose gel electrophoresis. Lanes: 1, 100-bp DNA ladder; 2, rJ2.2; 3, rJ2.2.CCL2; 4, rJ2.2.ΔCCL2. While the S gene was detected in all samples, the *CCL2* gene was detected only in the cells infected with rJ2.2.CCL2 or rJ2.2.ΔCCL2. (B) Sequence analysis showed that the *CCL2* gene amplified from rJ2.2.ΔCCL2-infected cells (lower panel) contained the introduced stop codon. (C) Expression of CCL2 protein was detected with anti-CCL2 antibody, as described in Materials and Methods. Whereas cells infected with rJ2.2, rJ2.2.CCL2, or rJ2.2.ΔCCL2 all expressed the viral N protein, CCL2 was detected only in cells infected with rJ2.2.CCL2.

## RESULTS

**Generation and characterization of rJ2.2.CCL2.** While mice infected with virulent stains of JHM, including JHM.SD, develop a uniformly fatal acute encephalitis, infection with the anti-S antibody escape variant J2.2-v-1 results in only 10 to 20% mortality. All survivors develop a subacute encephalomyelitis with demyelination present by 12 days postinoculation (p.i.) (19). Since nonrecombinant J2.2-v-1 was used in our previous studies of JHM-infected RAG1$^{-/-}$ mice, we first developed a recombinant version of this strain (rJ2.2) as described in Materials and Methods. B6 mice infected with 500 PFU rJ2.2 displayed a subacute encephalitis and clinical signs of demyelination at 12 days p.i. (data not shown). These results confirmed previous data showing that the L1114F change was critical for the diminished virulence of J2.2-v-1 (49, 51).

**Expression of CCL2 in rJ2.2.CCL2-infected cells.** Next, we generated a recombinant J2.2-v-1 that expressed CCL2 (rJ2.2.CCL2) (Fig. 1). We expected CCL2 to be functional because an exogenous CD8 T-cell epitope, gp33 derived from lymphocytic choriomeningitis virus, inserted into gene 4 was expressed and elicited a robust cytotoxic lymphocyte response in infected mice. Also, CXCL10 was expressed when inserted into gene 4 (5, 23, 48). As a control, a second recombinant virus was developed in which only a truncated CCL2 was encoded (rJ2.2.ΔCCL2) (Fig. 1). We detected *CCL2* mRNA in HeLa-MHVR cells infected with either rJ2.2.CCL2 or rJ2.2.ΔCCL2, but not in those infected with wild-type rJ2.2 (Fig. 2A). Sequence analysis confirmed that *CCL2* mRNA detected in cells infected with rJ2.2.ΔCCL2 contained the desired point mutation (A-to-T change at nucleotide 154) (Fig. 2B). Next, we examined the synthesis of CCL2 protein in infected cells (Fig. 2C). To enhance our ability to detect CCL2, infection of the cells was performed in the presence of brefeldin A to block the secretion of CCL2. All samples infected with either rJ2.2, rJ2.2.CCL2, or rJ2.2.ΔCCL2 supported viral replication as detected by staining with MAb directed against viral N protein (top panel). In contrast, CCL2 was detected only in those cells infected with rJ2.2.CCL2 virus (bottom panel).

The ability of the CCL2 expressed by rJ2.2.CCL2 to act as a macrophage chemoattractant was analyzed using a chemotaxis assay as described in Materials and Methods (Fig. 3). A small number of THP-1 cells migrated into the lower chamber in response to supernatants obtained from the cultures infected with either rJ2.2 or rJ2.2.ΔCCL2. In contrast, the number of cells that migrated in response to supernatants obtained from rJ2.2.CCL2-infected cells was fivefold greater ($P < 0.0002$). This increased migration occurred largely in response to CCL2, since preincubation for 30 min with anti-CCL2 neutralizing antibody (100 μg/ml) resulted in a greater than 50% reduction in the number of cells detected in the bottom chamber ($P < 0.0001$). Similar results were obtained when thioglycolate-elicited peritoneal macrophages were used in place of

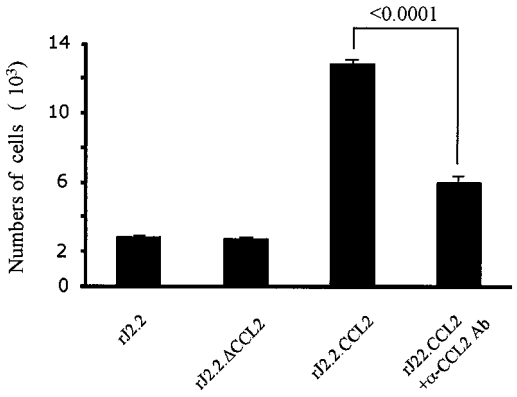


FIG. 3. Functional CCL2 was detected in the supernatants of cells infected with recombinant J2.2.CCL2. HeLa-MHVR cells were infected with rJ2.2, rJ2.2.CCL2, or rJ2.2.ΔCCL2 at an MOI of 0.5. Supernatants were harvested and analyzed as described in Materials and Methods. To confirm that CCL2 was responsible for the transmigration indicated in the figure, some samples were preincubated with anti-CCL2 antibody (100 μg/ml) for 30 min. THP-1 cells ($5 \times 10^5$ cells/well) were placed on the top chamber of a transwell plate and incubated for 2 h. After the migration period, adherent and nonadherent cells were collected from the lower chambers of the transwell plate and the number of cells determined by counting each cell population for 1 min in a FACScan flow cytometer. Samples were analyzed in quadriplicate. A representative example of three independent experiments is shown.

THP-1 cells (data not shown). These differences in chemoattractant activity were not due to differences in virus replication because there were no differences in virus growth kinetics in cells infected with either rJ2.2, rJ2.2.CCL2, or rJ2.2.ΔCCL2 (data not shown).

**CCL2 expression by rJ2.2.CCL2 consistently prolonged survival compared to rJ2.2.ΔCCL2-infected mice.** RAG1$^{-/-}$ mice infected with rJ2.2.ΔCCL2 exhibited clinical signs consistent with encephalitis, including lethargy, ruffled fur, and hunching, with death occurring between 10 and 14 days p.i. (Fig. 4A). In contrast, mice infected with rJ2.2.CCL2 remained asymptomatic until 11 days p.i. They then began to exhibit clinical signs consistent with demyelination, including tail and hindlimb paresis. Clinical disease progressed in the absence of complete virus clearance, resulting in hindlimb paralysis and the development of encephalitis. Viral titers in the brains of mice infected with rJ2.2.ΔCCL2 were slightly, but significantly, higher than those in mice infected with rJ2.2.CCL2 when analyzed at 12 to 14 days p.i. ($6.4 \pm 0.1$ versus $5.8 \pm 0.1$, respectively; $P < 0.001$) (Table 1).

**Demyelination was induced in rJ2.2.CCL2-infected RAG1$^{-/-}$ mice.** Infection of RAG1$^{-/-}$ mice with nonrecombinant J2.2-v-1 did not result in demyelination, despite high viral loads in the infected CNS. Since our results showed that infection with rJ2.2.CCL2 results in clinical disease consistent with demyelination (hindlimb paresis/paralysis), we next examined infected spinal cords for macrophage/microglia infiltration and myelin destruction. We detected only a small amount of demyelination in mice infected with rJ2.2.ΔCCL2 ($1.1 \pm 0.4\%$) (Fig. 5D and Table 1), virtually the same as that observed in RAG1$^{-/-}$ mice infected with nonrecombinant J2.2-v-1 (17). Consistent with this absence of demyelination, only small numbers of infiltrating macrophages/microglia were detected (Fig. 5E), although viral antigen was abundant in the gray and white matter (Fig. 5F).

In contrast, demyelination was readily detected in the white matter of rJ2.2.CCL2-infected mice ($14.6 \pm 2.4\%$) (Fig. 5A and Table 1) at days 12 to 14 p.i., with large numbers of F4/80-positive cells present at sites of myelin destruction (Fig. 5B). To quantify the number of macrophages/microglia in the spinal cords of mice infected with rJ2.2.CCL2 or rJ2.2.ΔCCL2, we counted the number of F4/80-positive cells as described in Materials and Methods (Table 1). There was an approximately threefold increase in the numbers of macrophages/microglia in the spinal cords of rJ2.2.CCL2-infected mice compared to

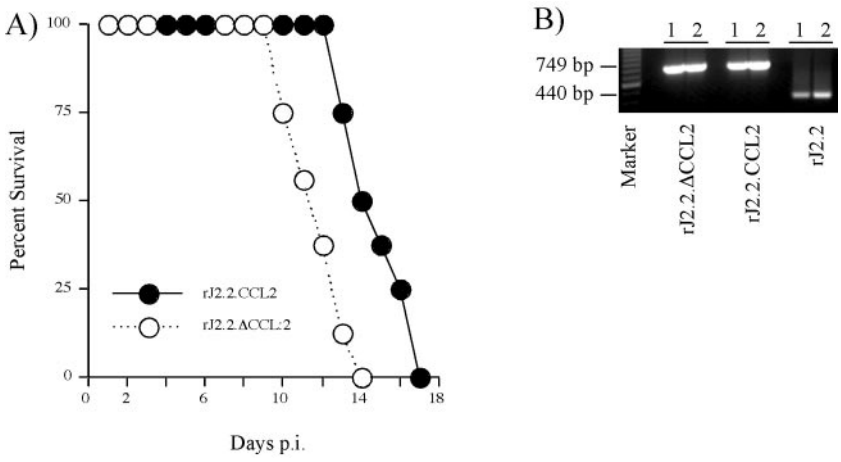


FIG. 4. Infection with rJ2.2.CCL2 resulted in delayed mortality compared to infection with rJ2.2.ΔCCL2. (A) Six-week-old RAG1$^{-/-}$ mice were infected i.c. with 500 PFU of either rJ2.2.CCL2 ($n = 12$) or rJ2.2.ΔCCL2 ($n = 16$). rJ2.2.CCL2-infected mice began to show clinical signs consistent with demyelination, including wobbly gait and hindlimb paresis, at 12 to 14 days p.i., and became moribund by 15 to 17 days p.i. In contrast, mice infected with rJ2.2.ΔCCL2 displayed signs consistent with encephalitis, including hunching, ruffled fur, and lethargy, at 9 to 11 days p.i. and became moribund by 14 days p.i. The fraction surviving at each day p.i. is shown. (B) To determine whether the *CCL2* gene was deleted from rJ2.2.CCL2 or rJ2.2.ΔCCL2 after passage in mice, RNA was analyzed by RT-PCR using primers that flanked the inserted sequence. Only full-length products were detected.

TABLE 1. Demyelination, viral titers, and macrophage/microglia in the CNS of rJ2.2-infected RAG1$^{-/-}$ mice at 12 to 14 days p.i.

| Virus | Demyelination (no.)[a] | Viral titers ($log_{10}$PFU/g brain) (no.)[a] | Macrophages per 1.25-mm-wide section[c] | | |
|---|---|---|---|---|---|
| | | | Gray matter | White matter | Total |
| rJ2.2.CCL2 | 14.6 ± 2.4%[b] (11) | 5.8 ± 0.1[b] (11) | 17.2 ± 0.7 | 50.3 ± 7.8[d] | 67.4 ± 7.9[d] |
| rJ2.2.ΔCCL2 | 1.1 ± 0.4% (8) | 6.4 ± 0.1 (8) | 16.6 ± 0.8 | 6.6 ± 1.5 | 23.2 ± 1.7 |

[a] Number of individual mice analyzed. Mice infected with rJ2.2.CCL2 or rJ2.2.ΔCCL2 were harvested at 13.1 ± 0.2 or 12.9 ± 0.3 days p.i., respectively.
[b] Values are significantly different from those for rJ2.2.ΔCCL2-infected mice: $P < 0.0003$ and $P < 0.001$, respectively.
[c] Numbers of macrophages/microglia infiltrating the CNS were quantified from three mice infected with rJ2.2.CCL2 and from three mice infected with rJ2.2.ΔCCL2 as described in Materials and Methods.
[d] values are significantly different from those for rJ2.2.ΔCCL2-infected mice: $P < 0.0002$ and $P < 0.006$, respectively.

those infected with rJ2.2.ΔCCL2. While similar numbers of F4/80-positive cells were observed in the gray matter of mice infected with either rJ2.2.CCL2 or rJ2.2.ΔCCL2, nearly 10-fold more F4/80-positive cells were detected in the white matter of mice infected with rJ2.2.CCL2 than in that of rJ2.2.ΔCCL2-infected mice. Viral antigen was absent from demyelinating lesions (Fig. 5A and C), supporting the notion that demyelination occurs as a consequence of the immune-mediated destruction of virus-infected cells. As in other models of JHM-induced demyelination (45), myelin loss in rJ2.2.CCL2-infected mice was primary (not secondary to axonal destruction), with intact axons detected by staining for phosphoneurofilament (Fig. 5G and H).

***CCL2* mRNA expression was elevated in the CNS of mice infected with rJ2.2.CCL2.** To assay *CCL2* mRNA expression in the infected CNS, we analyzed RNA harvested from the spinal cords of mice infected with rJ2.2.CCL2, rJ2.2.ΔCCL2, or rJ2.2 at 11 days p.i. by RNase protection assays as previously described (17) (data not shown). *CCL2* mRNA levels were approximately five- to sixfold higher in rJ2.2.CCL2- or rJ2.2.ΔCCL2-infected mice than those in mice infected with rJ2.2. Furthermore, there were no significant differences in the levels of MIP-2, *CCL4*/MIP-1β, *CCL5*, or *CCL7*/MCP-3 mRNA between mice infected with rJ2.2.CCL2 or rJ2.2ΔCCL2. This suggested that the greater macrophage/microglia infiltration observed in rJ2.2.CCL2-infected mice resulted directly from CCL2 overexpression and not secondarily from the CCL2-induced upregulation of another macrophage chemoattractant. Of note, more *CXCL10* mRNA was detected in rJ2.2ΔCCL2-infected mice than in those infected with rJ2.2CCL2, but this difference did not reach statistical significance.

**CCL2 sequence was not deleted in infected RAG1$^{-/-}$ mice.** Since exogenous genes inserted into gene 4 are sometimes deleted during murine infection (23, 43), we assayed these RNA samples by RT-PCR for the presence of deletions using primers that flanked the inserted sequence. Only a band corresponding to the undeleted CCL2 product was detected in mice infected with rJ2.2.CCL2 or rJ2.2.ΔCCL2 (Fig. 4B).

## DISCUSSION

Demyelination is not detected in J2.2-v-1-infected RAG1$^{-/-}$ mice in the absence of the adoptive transfer of virus-specific T cells or antibodies (55). Here, we show that neither T cells nor antibodies are required for demyelination if the expression of a single macrophage chemoattractant, CCL2, is upregulated in virus-infected cells. Elevated expression of CCL2 resulted in increased macrophage/microglia infiltration into the white matter of the spinal cord, presumably via CCL2/CCR2 interactions, which in turn resulted in virus clearance and demyelination. CCR2, the only known functional receptor for CCL2, is expressed on T cells, dendritic cells, astrocytes, neurons, and activated microglia as well as macrophages (1, 10, 31). While CCR2 is not expressed at significant levels on the surfaces of resting NK cells, it is upregulated after stimulation with cytokines, such as interleukin-2 or interleukin-15 (20, 40). Increased migration of NK cells may also contribute to demyelination in these mice, although we saw no difference in NK infiltration into the CNS when mice infected with rJ2.2.CCL2 or rJ2.2 ΔCCL2 were analyzed at 3 days p.i. (unpublished observations).

Infection with J2.2-v-1 induces a proinflammatory environment in the infected RAG1$^{-/-}$ CNS (17). This inflammatory milieu is critical for the development of demyelination, since multiple studies showed that transgenic expression of CCL2 in the central nervous system, lungs, or pancreas results in monocyte and lymphocyte recruitment to the organ expressing CCL2 but that these recruited cells are not activated in the absence of additional inflammatory stimuli, such as lipopolysaccharide treatment or infection (2, 4, 9, 14, 15). CCL2 is most likely expressed by astrocytes in the CNS of J2.2-v-1- or rJ2.2-infected mice, since these cells are the primary source for CCL2 in rodents with EAE or exposed to other CNS insults, including trauma and ischemia (11, 13). CCL2 is also expressed primarily by astrocytes in patients with multiple sclerosis (50). Infection with rJ2.2.CCL2 resulted in enhanced expression only in infected cells, which, in the case of J2.2-v-1, are predominantly oligodendrocytes and astrocytes (8). We attribute the increased demyelination that we observed in mice infected with J2.2.CCL2 to increased expression of the chemokine, but it is also possible that ectopic expression of CCL2 in oligodendrocytes contributed to this enhancement.

While virus-expressed CCL2 caused increased macrophage/microglia infiltration into the white matter of infected RAG1$^{-/-}$ mice, CCL2 is also critical for leukocyte infiltration into sites of infection in immunocompetent mice. CCR2$^{-/-}$ mice exhibit increased susceptibility to infection with pathogens such as *Mycobacterium tuberculosis*, *Listeria monocytogenes*, or *Cryptococcous neoformans* (26, 36, 46) with diminished infiltration of T cells and macrophages into the infected organs. However, at least in mice infected with *M. tuberculosis*, the critical defect is a lack of CCR2 expression by myeloid cells, since the expression of CCR2 on these cells restores both lymphocyte and monocyte recruitment to wild-type levels in

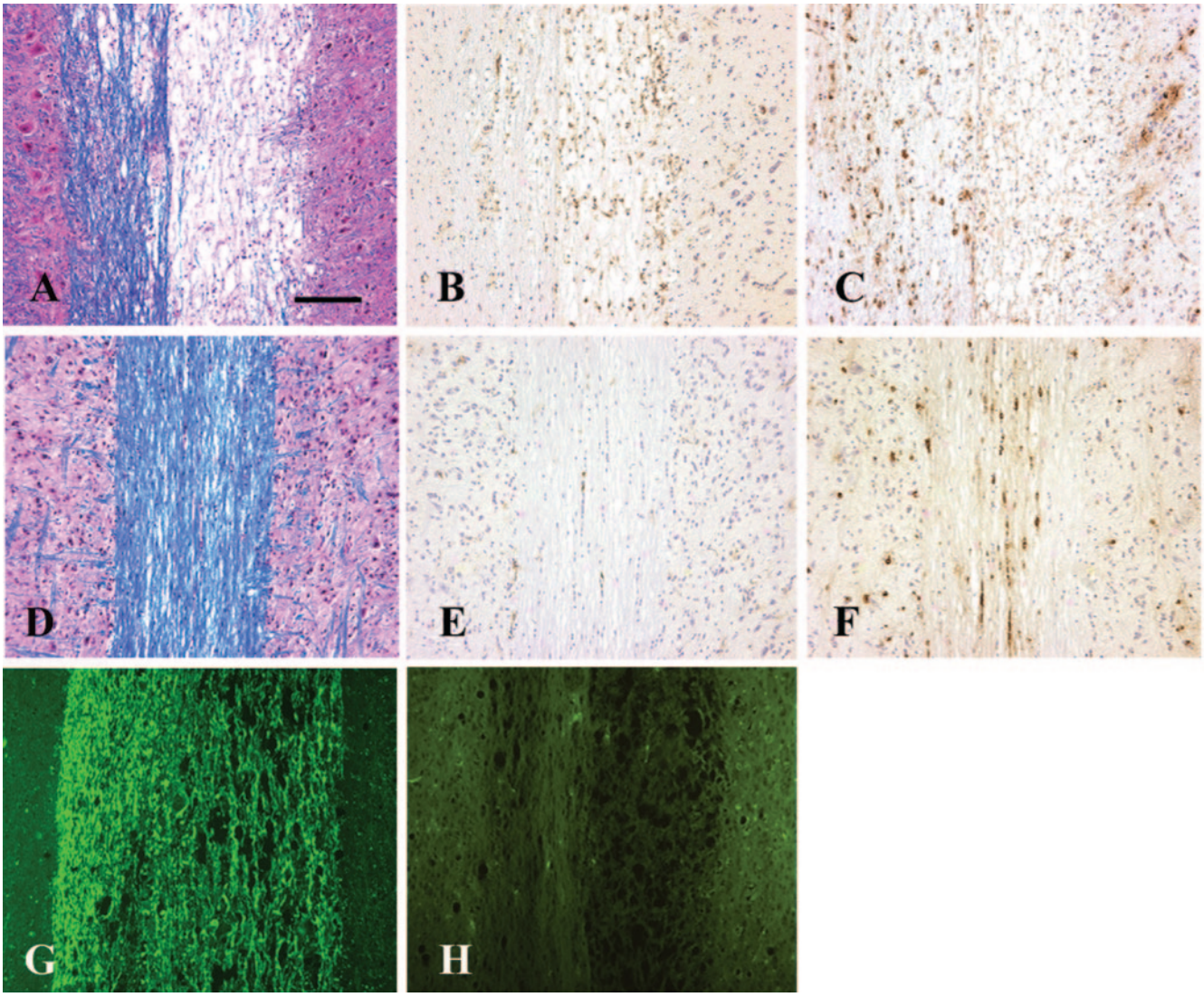


FIG. 5. Detection of demyelination in rJ2.2-infected RAG1$^{-/-}$ mice. RAG1$^{-/-}$ mice were infected i.c. with rJ2.2.CCL2 (A to C, G, and H) or rJ2.2.ΔCCL2 (D to F). Mice were harvested at 12 to 14 days p.i., and serial longitudinal sections (8 μm thick) of spinal cord were examined for demyelination (A and D), macrophage/microglia infiltration (B and E), and viral antigen (C and F) as described in Materials and Methods. Demyelination (A) and extensive macrophage/microglia infiltration into the white matter (B) were evident only in rJ2.2.CCL2-infected mice, but not in those infected with rJ2.2.ΔCCL2 (D and E). However, viral antigen was uniformly distributed throughout spinal cords in both rJ2.2.CCL2-infected (C) and rJ2.2.ΔCCL2-infected (F) mice, except in areas of demyelination (compare A and C). Axons were preserved (G) in areas of demyelination (A). No axonal staining was detected in the absence of anti-phosphoneurofilament antibody (H). Quantification of demyelination and the number of mice analyzed in these experiments are shown in Table 1. Scale bar, 250 μm.

the lungs of infected animals (35). CCL2/CCR2 interactions may also contribute to neuropathogenesis independent of directly effecting leukocyte migration. CCL2 stimulates blood monocytes and microglia to secrete matrix metalloproteinases-9 and -19 (6, 42), which facilitate additional monocyte/macrophage migration into the CNS by degrading basement membrane and extracellular matrix components.

In summary, our results show that demyelination in the J2.2-v-1-infected RAG1$^{-/-}$ mouse requires only enhanced expression of a single macrophage chemoattractant in the context of a proinflammatory milieu. The elimination of the adaptive immune response from the demyelinating process in rJ2.2.CCL2-infected mice should make it possible to determine the minimal requirements for myelin destruction.

## ACKNOWLEDGMENTS

We thank John Harty for critical review of the manuscript and Katherine O'Malley and Lecia Pewe for technical assistance.

This work was supported in part by grants from the NIH (NS 40438) and National Multiple Sclerosis Society (RG 2864).

## REFERENCES

1. **Banisadr, G., F. Queraud-Lesaux, M. C. Boutterin, D. Pelaprat, B. Zalc, W. Rostene, F. Haour, and S. M. Parsadaniantz.** 2002. Distribution, cellular localization and functional role of CCR2 chemokine receptors in adult rat brain. J. Neurochem. **81:**257–269.

2. **Bennett, J. L., A. Elhofy, M. C. Canto, M. Tani, R. M. Ransohoff, and W. J. Karpus.** 2003. CCL2 transgene expression in the central nervous system directs diffuse infiltration of CD45(high)CD11b(+) monocytes and enhanced Theiler's murine encephalomyelitis virus-induced demyelinating disease. J. Neurovirol. **9:**623–636.
3. **Chen, B. P., W. A. Kuziel, and T. E. Lane.** 2001. Lack of CCR2 results in increased mortality and impaired leukocyte activation and trafficking following infection of the central nervous system with a neurotropic coronavirus. J. Immunol. **167:**4585–4592.
4. **Chen, Y., J. M. Hallenbeck, C. Ruetzler, D. Bol, K. Thomas, N. E. Berman, and S. N. Vogel.** 2003. Overexpression of monocyte chemoattractant protein 1 in the brain exacerbates ischemic brain injury and is associated with recruitment of inflammatory cells. J. Cereb. Blood Flow Metab. **23:**748–755.
5. **Chua, M. M., K. C. MacNamara, L. San Mateo, H. Shen, and S. R. Weiss.** 2004. Effects of an epitope-specific $CD8^+$ T-cell response on murine coronavirus central nervous system disease: protection from virus replication and antigen spread and selection of epitope escape mutants. J. Virol. **78:**1150–1159.
6. **Cross, A. K., and M. N. Woodroofe.** 1999. Chemokine modulation of matrix metalloproteinase and TIMP production in adult rat brain microglia and a human microglial cell line in vitro. Glia **28:**183–189.
7. **Dandekar, A. A., D. Anghelina, and S. Perlman.** 2004. Bystander CD8 T-cell-mediated demyelination is interferon-gamma-dependent in a coronavirus model of multiple sclerosis. Am. J. Pathol. **164:**363–369.
8. **Fleming, J. O., M. D. Trousdale, J. Bradbury, S. A. Stohlman, and L. P. Weiner.** 1987. Experimental demyelination induced by coronavirus JHM (MHV-4): molecular identification of a viral determinant of paralytic disease. Microb. Pathog. **3:**9–20.
9. **Fuentes, M. E., S. K. Durham, M. R. Swerdel, A. C. Lewin, D. S. Barton, J. R. Megill, R. Bravo, and S. A. Lira.** 1995. Controlled recruitment of monocytes and macrophages to specific organs through transgenic expression of monocyte chemoattractant protein-1. J. Immunol. **155:**5769–5776.
10. **Galasso, J. M., M. J. Miller, R. M. Cowell, J. K. Harrison, J. S. Warren, and F. S. Silverstein.** 2000. Acute excitotoxic injury induces expression of monocyte chemoattractant protein-1 and its receptor, CCR2, in neonatal rat brain. Exp. Neurol. **165:**295–305.
11. **Glabinski, A. R., M. Tani, R. M. Strieter, V. K. Tuohy, and R. M. Ransohoff.** 1997. Synchronous synthesis of alpha- and beta-chemokines by cells of diverse lineage in the central nervous system of mice with relapses of chronic experimental autoimmune encephalomyelitis. Am. J. Pathol. **150:**617–630.
12. **Glabinski, A. R., M. Tani, V. K. Tuohy, R. J. Tuthill, and R. M. Ransohoff.** 1995. Central nervous system chemokine mRNA accumulation follows initial leukocyte entry at the onset of acute murine experimental autoimmune encephalomyelitis. Brain Behav. Immun. **9:**315–330.
13. **Gourmala, N. G., M. Buttini, S. Limonta, A. Sauter, and H. W. Boddeke.** 1997. Differential and time-dependent expression of monocyte chemoattractant protein-1 mRNA by astrocytes and macrophages in rat brain: effects of ischemia and peripheral lipopolysaccharide administration. J. Neuroimmunol. **74:**35–44.
14. **Grewal, I. S., B. J. Rutledge, J. A. Fiorillo, L. Gu, R. P. Gladue, R. A. Flavell, and B. J. Rollins.** 1997. Transgenic monocyte chemoattractant protein-1 (MCP-1) in pancreatic islets produces monocyte-rich insulitis without diabetes: abrogation by a second transgene expressing systemic MCP-1. J. Immunol. **159:**401–408.
15. **Gunn, M. D., N. A. Nelken, X. Liao, and L. T. Williams.** 1997. Monocyte chemoattractant protein-1 is sufficient for the chemotaxis of monocytes and lymphocytes in transgenic mice but requires an additional stimulus for inflammatory activation. J. Immunol. **158:**376–383.
16. **Haring, J. S., and S. Perlman.** 2003. Bystander CD4 T cells do not mediate demyelination in mice infected with a neurotropic coronavirus. J. Neuroimmunol. **137:**42–50.
17. **Haring, J. S., L. L. Pewe, and S. Perlman.** 2002. Bystander CD8 T cell-mediated demyelination after viral infection of the central nervous system. J. Immunol. **169:**1550–1555.
18. **Hemmer, B., J. J. Archelos, and H. P. Hartung.** 2002. New concepts in the immunopathogenesis of multiple sclerosis. Nat. Rev. Neurosci. **3:**291–301.
19. **Houtman, J. J., and J. O. Fleming.** 1996. Dissociation of demyelination and viral clearance in congenitally immunodeficient mice infected with murine coronavirus JHM. J. Neurovirol. **2:**101–110.
20. **Inngjerdingen, M., B. Damaj, and A. A. Maghazachi.** 2001. Expression and regulation of chemokine receptors in human natural killer cells. Blood **97:** 367–375.
21. **Izikson, L., R. S. Klein, A. D. Luster, and H. L. Weiner.** 2002. Targeting monocyte recruitment in CNS autoimmune disease. Clin. Immunol. **103:** 125–131.
22. **Karpus, W. J., and R. M. Ransohoff.** 1998. Chemokine regulation of experimental autoimmune encephalomyelitis: temporal and spatial expression patterns govern disease pathogenesis. J. Immunol. **161:**2667–2671.
23. **Kim, T. S., and S. Perlman.** 2003. Protection against CTL escape and clinical disease in a murine model of virus persistence. J. Immunol. **171:**2006–2013.
24. **Kim, T. S., and S. Perlman.** 2005. Virus-specific antibody, in the absence of T cells, mediates demyelination in mice infected with a neurotropic coronavirus. Am. J. Pathol. **166:**801–809.
25. **Kuo, L., G.-J. Godeke, M. J. B. Raamsman, P. S. Masters, and P. J. M. Rottier.** 2000. Retargeting of coronavirus by substitution of the spike glycoprotein ectodomain: crossing the host cell species barrier. J. Virol. **74:**1393–1406.
26. **Kurihara, T., G. Warr, J. Loy, and R. Bravo.** 1997. Defects in macrophage recruitment and host defense in mice lacking the CCR2 chemokine receptor. J. Exp. Med. **186:**1757–1762.
27. **Lane, T. E., M. T. Liu, B. P. Chen, V. C. Asensio, R. M. Samawi, A. D. Paoletti, I. L. Campbell, S. L. Kunkel, H. S. Fox, and M. J. Buchmeier.** 2000. A central role for $CD4^+$ T cells and RANTES in virus-induced central nervous system inflammation and demyelination. J. Virol. **74:**1415–1424.
28. **Liu, M. T., D. Armstrong, T. A. Hamilton, and T. E. Lane.** 2001. Expression of Mig (monokine induced by interferon-gamma) is important in T lymphocyte recruitment and host defense following viral infection of the central nervous system. J. Immunol. **166:**1790–1795.
29. **Liu, M. T., B. P. Chen, P. Oertel, M. J. Buchmeier, D. Armstrong, T. A. Hamilton, and T. E. Lane.** 2000. The T cell chemoattractant IFN-inducible protein 10 is essential in host defense against viral-induced neurologic disease. J. Immunol. **165:**2327–2330.
30. **Mahad, D. J., and R. M. Ransohoff.** 2003. The role of MCP-1 (CCL2) and CCR2 in multiple sclerosis and experimental autoimmune encephalomyelitis (EAE). Semin. Immunol. **15:**23–32.
31. **Ontiveros, E., T. S. Kim, T. M. Gallagher, and S. Perlman.** 2003. Enhanced virulence mediated by the murine coronavirus, mouse hepatitis virus strain JHM, is associated with a glycine at residue 310 of the spike glycoprotein. J. Virol. **77:**10260–10269.
32. **Ontiveros, E., L. Kuo, P. S. Masters, and S. Perlman.** 2001. Inactivation of expression of gene 4 of mouse hepatitis virus strain JHM does not affect virulence in the murine CNS. Virology **289:**230–238.
33. **Perlman, S.** 1998. Pathogenesis of coronavirus-induced infections. Review of pathological and immunological aspects. Adv. Exp. Med. Biol. **440:**503–513.
34. **Perlman, S., R. Schelper, E. Bolger, and D. Ries.** 1987. Late onset, symptomatic, demyelinating encephalomyelitis in mice infected with MHV-JHM in the presence of maternal antibody. Microb. Pathog. **2:**185–194.
35. **Peters, W., J. G. Cyster, M. Mack, D. Schlondorff, A. J. Wolf, J. D. Ernst, and I. F. Charo.** 2004. CCR2-dependent trafficking of F4/80dim macrophages and CD11cdim/intermediate dendritic cells is crucial for T cell recruitment to lungs infected with Mycobacterium tuberculosis. J. Immunol. **172:**7647–7653.
36. **Peters, W., H. M. Scott, H. F. Chambers, J. L. Flynn, I. F. Charo, and J. D. Ernst.** 2001. Chemokine receptor 2 serves an early and essential role in resistance to Mycobacterium tuberculosis. Proc. Natl. Acad. Sci. USA **98:** 7958–7963.
37. **Pewe, L., J. Haring, and S. Perlman.** 2002. CD4 T-cell-mediated demyelination is increased in the absence of gamma interferon in mice infected with mouse hepatitis virus. J. Virol. **76:**7329–7333.
38. **Pewe, L., G. Wu, E. M. Barnett, R. Castro, and S. Perlman.** 1996. Cytotoxic T cell-resistant variants are selected in a virus-induced demyelinating disease. Immunity **5:**253–262.
39. **Pewe, L. L., and S. Perlman.** 2002. Cutting edge: CD8 T cell-mediated demyelination is IFN-gamma dependent in mice infected with a neurotropic coronavirus. J. Immunol. **168:**1547–1551.
40. **Polentarutti, N., P. Allavena, G. Bianchi, G. Giardina, A. Basile, S. Sozzani, A. Mantovani, and M. Introna.** 1997. IL-2-regulated expression of the monocyte chemotactic protein-1 receptor (CCR2) in human NK cells: characterization of a predominant 3.4-kilobase transcript containing CCR2B and CCR2A sequences. J. Immunol. **158:**2689–2694.
41. **Ransohoff, R. M., P. Kivisakk, and G. Kidd.** 2003. Three or more routes for leukocyte migration into the central nervous system. Nat. Rev. Immunol. **3:**569–581.
42. **Robinson, S. C., K. A. Scott, and F. R. Balkwill.** 2002. Chemokine stimulation of monocyte matrix metalloproteinase-9 requires endogenous TNF-alpha. Eur. J. Immunol. **32:**404–412.
43. **Sarma, J. D., E. Scheen, S. H. Seo, M. Koval, and S. R. Weiss.** 2002. Enhanced green fluorescent protein expression may be used to monitor murine coronavirus spread in vitro and in the mouse central nervous system. J. Neurovirol. **8:**381–391.
44. **Sorensen, T. L., M. Tani, J. Jensen, V. Pierce, C. Lucchinetti, V. A. Folcik, S. Qin, J. Rottman, F. Sellebjerg, R. M. Strieter, J. L. Frederiksen, and R. M. Ransohoff.** 1999. Expression of specific chemokines and chemokine receptors in the central nervous system of multiple sclerosis patients. J. Clin. Investig. **103:**807–815.
45. **Stohlman, S. A., and D. R. Hinton.** 2001. Viral induced demyelination. Brain Pathol. **11:**92–106.
46. **Traynor, T. R., A. C. Herring, M. E. Dorf, W. A. Kuziel, G. B. Toews, and G. B. Huffnagle.** 2002. Differential roles of CC chemokine ligand 2/monocyte chemotactic protein-1 and CCR2 in the development of T1 immunity. J. Immunol. **168:**4659–4666.
47. **Trifilo, M. J., C. C. Bergmann, W. A. Kuziel, and T. E. Lane.** 2003. CC chemokine ligand 3 (CCL3) regulates $CD8^+$-T-cell effector function and migration following viral infection. J. Virol. **77:**4004–4014.
48. **Trifilo, M. J., C. Montalto-Morrison, L. N. Stiles, K. R. Hurst, J. L. Hardison, J. E. Manning, P. S. Masters, and T. E. Lane.** 2004. CXC chemokine ligand 10 controls viral infection in the central nervous system: evidence for

a role in innate immune response through recruitment and activation of natural killer cells. J. Virol. **78:**585–594.
49. **Tsai, J. C., L. de Groot, J. D. Pinon, K. T. Iacono, J. J. Phillips, S. H. Seo, E. Lavi, and S. R. Weiss.** 2003. Amino acid substitutions within the heptad repeat domain 1 of murine coronavirus spike protein restrict viral antigen spread in the central nervous system. Virology **312:**369–380.
50. **Van Der Voorn, P., J. Tekstra, R. H. Beelen, C. P. Tensen, P. Van Der Valk, and C. J. De Groot.** 1999. Expression of MCP-1 by reactive astrocytes in demyelinating multiple sclerosis lesions. Am. J. Pathol. **154:**45–51.
51. **Wang, F., J. O. Fleming, and M. M. C. Lai.** 1992. Sequence analysis of the spike protein gene of murine coronavirus variants: study of genetic sites affecting neuropathogenicity. Virology **186:**742–749.
52. **Wang, F., S. A. Stohlman, and J. O. Fleming.** 1990. Demyelination induced by murine hepatitis virus JHM strain (MHV-4) is immunologically mediated. J. Neuroimmunol. **30:**31–41.
53. **Weiss, J. M., S. A. Downie, W. D. Lyman, and J. W. Berman.** 1998. Astrocyte-derived monocyte-chemoattractant protein-1 directs the transmigration of leukocytes across a model of the human blood-brain barrier. J. Immunol. **161:**6896–6903.
54. **Wu, G. F., A. A. Dandekar, L. Pewe, and S. Perlman.** 2000. CD4 and CD8 T cells have redundant but not identical roles in virus-induced demyelination. J. Immunol. **165:**2278–2286.
55. **Wu, G. F., and S. Perlman.** 1999. Macrophage infiltration, but not apoptosis, is correlated with immune-mediated demyelination following murine infection with a neurotropic coronavirus. J. Virol. **73:**8771–8780.